

## HIGHLY-IONIZED SPECIES IN THE INTERSTELLAR MEDIUM

J. H. BLACK,<sup>1</sup> A. K. DUPREE,<sup>1</sup> L. W. HARTMANN, AND J. C. RAYMOND

Harvard-Smithsonian Center for Astrophysics

Received 1979 October 22; accepted 1980 January 29

### ABSTRACT

Interstellar absorption lines have been observed toward 25 stars with the *International Ultraviolet Explorer* satellite. Results are presented for observations of interstellar lines of C III, C IV, N V, Si III, and Si IV. Strong lines of Si IV or C IV are seen toward 11 stars. The strengths of these lines are inconsistent with their formation in the same hot gas responsible for the interstellar O IV lines observed with the *Copernicus* ultraviolet spectrometer.

Comparison with simple models of the ionization structures of H II regions around hot stars suggests that the observed column densities of Si III, Si IV, and C IV are in harmony with those expected in normal photoionized nebulae.

The line of sight to HD 93250, an O3 V star near  $\eta$  Carinae, passes through highly ionized gas that shows features spanning  $250 \text{ km s}^{-1}$  in radial velocity.

Stellar wind velocities are presented for 21 of the stars observed in this survey of interstellar absorption lines.

*Subject headings:* interstellar: abundances — interstellar: matter — stars: winds — ultraviolet: spectra

### 1. INTRODUCTION

Even though most of the interstellar gas consists of cold atoms and molecules that are neutral or singly-ionized, observations of interstellar absorption lines in the ultraviolet have revealed measurable concentrations of highly-ionized species in many directions. Resonance lines of C IV, N V, Si III, and Si IV can be observed at high dispersion with the *International Ultraviolet Explorer* (IUE) satellite observatory. We have performed a survey of interstellar absorption lines in the wavelength region 1150–3200 Å toward 25 early-type stars. Along the lines of sight to 11 of these stars, we observe very strong, narrow absorption lines of Si IV and C IV. Lines of N V appear in eight directions. The N V lines may arise in the same gas responsible for the ubiquitous interstellar lines of O VI observed previously by the *Copernicus* spectrometer, but the lines of Si IV and C IV must be formed elsewhere. The lines of Si IV and C IV appear in the spectra of the stars of earliest spectral type in our sample. The strengths of the lines of Si III, Si IV, and C IV are compared with those predicted for simple models of photoionized nebulae. The observations are consistent with the formation of the lines in normal H II regions ionized by the very stars used to make the absorption line measurements.

At large distances from the galactic plane, highly-ionized species may be widely distributed and not confined to nebulae. Savage and de Boer (1979) have

recently used IUE to observe interstellar lines of Si IV and C IV toward hot stars in the Large Magellanic Cloud, and they interpret highly-redshifted galactic absorption in these lines as strong evidence for a galactic corona.

Interstellar lines of O VI have been observed with the Princeton ultraviolet spectrometer on the *Copernicus* satellite (Rogerson *et al.* 1973; York 1974; Jenkins and Meloy 1974). There are also *Copernicus* observations of interstellar Si III (Cohn and York 1977; Cowie and York 1978*a, b*). Careful analysis of the O VI lines (Jenkins 1978*a, b*) suggests that this highly-ionized material is truly interstellar, ubiquitous, and probably maintained collisionally in hot gas at temperatures  $T \gtrsim 10^5 \text{ K}$ . Velocity structures in O VI and Si III tend to be correlated in a sample of stars observed with *Copernicus* (Cowie *et al.* 1979). Highly-ionized gas in the vicinity of the Orion OB1 association covers a very broad range of radial velocities, and has been ascribed to an explosive event (e.g., a supernova) in the association (Cowie, Songaila, and York 1979).

There exist two types of competing interpretations of the O VI lines: these can be termed global and circumstellar. In both, O VI is produced by collisional ionization at temperatures  $T \gtrsim 10^5 \text{ K}$ . Global models envision a very hot ( $T = 10^5\text{--}10^6 \text{ K}$ ) coronal component of the interstellar medium which is maintained by the introduction of mechanical energy from occasional supernova shock waves. Depending upon the details of the propagation of these shocks through an inhomogeneous medium, the coronal gas may occupy narrow "tunnels" between large clouds (Cox and Smith 1974; Smith 1977) or it may effectively surround

<sup>1</sup> Guest Investigator with the *International Ultraviolet Explorer* satellite, which is sponsored and operated by the National Aeronautics and Space Administration, by the Science Research Council of the United Kingdom and by the European Space Agency.

numerous small clouds (McKee and Ostriker 1977). In the latter model, the O VI absorption lines arise in the conductive interfaces between cold clouds and hot coronal gas (McKee and Cowie 1977*a, b*). The circumstellar models (Castor, McCray, and Weaver 1975; Weaver *et al.* 1977) propose that the hot gas responsible for the O VI lines arises from the interaction between strong stellar winds and surrounding interstellar gas. It is significant that these models of "circumstellar bubbles" naturally incorporate a severe observational selection effect. Early-type stars must necessarily be used to provide background light sources for studies of interstellar absorption lines in the ultraviolet. The majority of luminous, hot stars also possess strong stellar winds whose velocities often exceed  $1000 \text{ km s}^{-1}$ . Elaborate statistical tests must be used in order to determine whether the data are in better agreement with global or circumstellar explanations (Jenkins 1978*a, b*). The respective merits of these models have been reviewed by Jenkins (1977, 1978*c*), McKee (1977), and McCray (1977). The contribution of the proposed coronal gas to the X-ray background has been discussed recently by Burstein *et al.* (1977). The sensitivity and wavelength coverage of *IUE* permit the measurement of the abundance and distribution of interstellar C IV and Si IV, ions which have not been widely accessible to previous instruments. Bruhweiler, Kondo, and McCluskey (1979) have recently observed narrow lines of Si IV and C IV with *IUE* toward  $\gamma^2$  Vel which they attribute to moderately hot ( $T \approx 40,000 \text{ K}$ ), collisionally-ionized gas associated with the Gum Nebula.

## II. OBSERVATIONS

### *a) Instrumental Performance*

The scientific instrument of the *IUE* Observatory is a 0.4 meter Cassegrain telescope that supplies light to two échelle spectrographs. The design and performance of the instrument have been described in detail by Boggess *et al.* (1978*a, b*). All observations reported in this paper were made with the short-wavelength prime (SWP) camera in the high-dispersion mode. With the exception of a single spectrum of  $\rho$  Oph, all exposures were made with the small (3" diameter) entrance aperture. The short-wavelength camera covers the range 1150–2100 Å with a constant resolving power  $R = 1.2 \times 10^4$  (Boggess *et al.* 1978*b*). This value of  $R$  is confirmed by the present data. The interstellar line of Cl I  $\lambda 1347.240$  is unsaturated in many of our spectra, and its usual full-width at half-peak,  $\Delta\lambda = 0.11 \text{ Å}$ , is a good indicator of the actual instrumental resolution.

A discussion of the precision of measurements made with *IUE* spectra is complicated by the variety of sources of noise (Boggess 1978*b*). A severe limitation upon interstellar line studies is imposed by the finite dynamic range of the detectors which consist of ultraviolet-to-visible converters coupled to television cameras. Under good observing conditions (i.e., dur-

ing those parts of the orbit in which the satellite is least affected by passage through the Earth's outer belt of energetic electrons) and at the optimum exposure level, the maximum signal-to-noise ratio is about 20 per resolution element at the level of one standard deviation ( $\sigma$ ). The minimum measurable equivalent width of a narrow line at wavelength  $\lambda$  is thus approximately

$$W_{\min} = \frac{3 \lambda}{20 R},$$

in a single exposure at the level of  $3\sigma$ . At  $\lambda = 1350 \text{ Å}$ , for example,  $W_{\min} = 0.017 \text{ Å}$ . The wavelength dependences of instrumental response, of intrinsic stellar fluxes, and of interstellar extinction generally ensure that no single spectral image is optimally exposed at all wavelengths. In order to study interstellar lines having equivalent widths less than  $0.02 \text{ Å}$ , it is necessary to combine several different exposures. In practice, we find that the effective signal-to-noise ratio increases with the number of exposures averaged, for small numbers of spectra (one to five). During the extraction of spectral data from the camera images, the continuum intensity is subjected to additional uncertainty through the subtraction of background. Such uncertainties are most severe at the shortest wavelengths where the échelle orders are most crowded, because the intensity in each order contains some contribution from adjacent orders. In practice, the establishment of the local zero-level for the continuum is rarely in error by more than 10%, but this uncertainty is propagated directly to the equivalent widths. All of the raw data have been handled with the standard procedures used by the image processing division of the *IUE* Observatory at Goddard Space Flight Center (GSFC). The measurements reported here result from further processing of the extracted spectra supplied on magnetic tapes by GSFC.

After completing the first version of this paper, we learned that all of the short-wavelength spectra used in this study had been processed with an erroneous intensity-transfer function (ITF). The nature of the error is that the intensities assigned to measured detector exposure levels are too large by factors up to 1.63 in a restricted range of exposure levels. Hence, wherever the exposure level of the gross spectrum or of the background lies within the affected range, intensities and equivalent widths will be incorrect. Well-exposed spectra with low backgrounds are largely unaffected by this error. The vicinities of the Si IV and C IV lines in many of our spectra are not affected severely by use of the incorrect ITF. Because it is not feasible to reprocess high-dispersion images, we are unable to present "corrected" intensities and equivalent widths; however, we have estimated the maximum possible errors in equivalent widths for all of the spectra. If the background exposure level lies in the affected range, then the continuum intensity level will be in error (because the zero-level is incorrect), and this error will be propagated to any equivalent width. Sixteen of our spectra suffer such errors in zero-level;

however, in nine of these cases, we have additional unaffected spectra of the same stars. Additionally, for six stars, the exposure levels in the spectra themselves near the Si IV and C IV lines lie in the affected range. For the two cases in which the maximum errors exceed 25%, additional unaffected spectra exist.

### b) The Observing Program

Twenty-five stars ranging in spectral type from B8 to O3 have been observed in this survey of interstellar absorption lines. The properties of these stars are summarized in Table 1. The columns list the HD catalogue number and common name, galactic coordinates, spectral classification,  $V$  magnitude,  $(B - V)$  color index, adopted color excess, projected rotational velocity  $v \sin i$ , associated H II regions and distance. These properties come from various published sources. Resonance lines of N V, C IV, and Si IV in many of the stellar spectra show strong P Cygni profiles indicating substantial rates of mass loss through stellar winds. The terminal velocity of the wind is estimated from the offset in wavelength of the limit of the blueward wing from the apparent rest wavelength of the stellar line. These terminal velocities are listed in Table 2. We generally find very good agreement with terminal velocities determined from *Copernicus* spectra (Snow and Morton 1976).

All of the stars in Table 1 were observed in the full spectral range  $\lambda\lambda 1150\text{--}3200$  of both spectrographs,

and many of them were observed several times to permit measurement of weak lines. The observations were made during 1978 April 24–27 and 1978 September 20–27. The stars of Table 1 were selected to cover a range of galactic coordinates and amounts of interstellar extinction. They do not constitute an unbiased sample because many were chosen specifically for their high probabilities of showing interesting interstellar line spectra. These stars are predominantly of very early spectral type, extremely luminous, and often highly reddened.

### c) Data Analysis

The velocity resolution of *IUE* spectra is about  $25 \text{ km s}^{-1}$ . This often exceeds the width of a narrow line and thus makes it difficult to obtain information about interstellar absorption directly from line profiles. Much of our information is derived from the equivalent widths of the lines. A small part of an order, typically a  $3 \text{ \AA}$  segment around the expected position of a line, is analyzed at a time. The intensities on either side of the line are fit by a least-squares technique with a polynomial function (ordinarily a straight line suffices) which serves as the continuum intensity  $I_c(\lambda)$ . An element of equivalent width

$$\Delta W_i = [1 - I(\lambda_i)/I_c(\lambda_i)]\delta\lambda_i,$$

is determined from the measured intensity  $I(\lambda_i)$  for each sampling interval  $i$  of width  $\delta\lambda_i$ . The total

TABLE 1  
OBSERVING LIST

HD Number	Star Name	$l^{\text{II}}$	$b^{\text{II}}$	Spectral Type	$V$	$B - V$	$E(B - V)$	$v \sin i$ (km s $^{-1}$ )	Distance (pc)	Associated H II Region
13854	...	134.38	-3.91	B1 Iab	6.49	+0.28	0.50	67	1760	...
23180	$\sigma$ Per	160.36	-17.74	B1 III	3.82	+0.06	0.30	75/150	265	...
23408	20 Tau	166.17	-23.53	B8 III	3.87	-0.07	0.000	38	80	...
23480	23 Tau	166.57	-23.77	B6 IV	4.18	-0.06	0.08	294	80	...
30614	$\alpha$ Cam	144.07	+14.04	O9.5 Ia	4.29	+0.04	0.34	95	800	...
36861	$\lambda$ Ori	195.05	-11.99	O8 III(f)	3.66	-0.19	0.12	75	575	S264
36879	...	185.22	-5.89	O7.5 III	7.56	+0.22	0.54	...	1940	...
38666	$\mu$ Col	237.29	-27.10	O9 V	5.16	-0.29	0.02	108	760	...
41117	$\chi^2$ Ori	189.69	-0.86	B2 Ia	4.63	+0.27	0.45	29	1040	...
46223	...	206.44	-2.07	O4 Vf	7.25	+0.22	0.54	143	1560	Rosette Neb.
57060	UW CMa	237.82	-5.37	O8.5 If	4.90	+0.14	0.45	136	1000	S310
57061	$\tau$ CMa	238.18	-5.54	O9 I	4.39	-0.14	0.17	120	1000	S310
91316	$\rho$ Leo	234.89	+52.77	B1 Ib	3.85	-0.14	0.08	69	1050	...
93250	...	287.51	-0.54	O3 Vf	7.38	+0.15	0.48	...	3220	Carina Neb.
112244	...	303.55	+6.03	O9.5 Ia	5.40	+0.04	0.34	138	1640	...
147933/4	$\rho$ Oph	353.69	+17.69	B3 V	4.63	+0.22	0.42	303	100	...
148937	...	336.37	-0.22	O6 f	6.71	+0.34	0.66	...	1600	RCW 108
149404	...	340.54	+3.01	O9 I	5.58	+0.43	0.74	...	780	...
151804	...	343.62	+1.94	O8 If	5.22	+0.07	0.38	...	1310	RCW 113
152424	...	343.36	+0.89	O9 I	6.27	+0.39	0.70	...	1250	RCW 113
203064	68 Cyg	87.61	-3.84	O8 V	4.99	0.00	0.31	328	510	S119
209975	19 Cep	104.87	+5.39	O9.5 I	5.10	+0.09	0.39	33	970	...
212571	$\pi$ Aqr	66.01	-44.74	B1 Vpe	4.68	-0.06	0.20	278	230	...
213087	26 Cep	108.50	+6.39	B0.5 Ib	5.46	+0.37	0.62	...	730	S150 (?)
218376	A Cas	109.95	-0.78	B0.5 IV	4.87	-0.04	0.24	74	490	...

TABLE 2  
SPECTRAL TERMINAL VELOCITIES

HD NUMBER	TERMINAL VELOCITY (km s <sup>-1</sup> )			TERMINAL
	N v	Si iv	C iv	
13854 .....	...	1120	1300	...
23180 .....	...	485	...	...
30614 .....	1770 (1890) <sup>a</sup>	1830 (1760, 2100)	1980	(1890)
36861 .....	...	250 (?)	...	(3050)
36879 .....	...	...	1590	...
38666 .....	...	...	...	...
41117 .....	...	810	720	...
46223 .....	...	...	3040	...
57060 .....	1900 (1630)	1490 (1230, 1450)	1690 (1550)	(1480)
57061 .....	(2380)	(2140)	2270	(2260)
91316 .....	(1800)	1270 (1620, 1530)	1200	(1580)
93250 .....	...	...	3280	...
112244 .....	1940 (1920)	1930	2270	(1900)
148937 .....	...	...	2360	...
149404 .....	...	2570	2770	...
151804 .....	1770 (1850)	1820	2190	(1850)
152424 .....	...	1800	1880	...
203064 .....	2860	2530	3330	...
209975 .....	2010	2060	2360	...
212571 .....	...	750	620	...
213087 .....	...	1830	2170	...

<sup>a</sup> Entries in parentheses are from Snow and Morton (1976).

equivalent width of the feature is merely the sum

$$W_\lambda = \sum_i \Delta W_i,$$

The statistical uncertainty of the least-squares fit to the continuum is a measure of the local rms noise in the spectrum, and is used to establish a formal error for each measurement of  $W_\lambda$ . In general this measured error is in harmony with the predicted uncertainty discussed in § IIa.

When several independent exposures are used, the relevant spectral regions are usually averaged before the equivalent width is determined. As long as a line is strong enough to be measured in a single exposure, there is no appreciable difference between  $W_\lambda$  determined from an averaged spectrum and the average of the values of  $W_\lambda$  measured from each exposure individually. Summing exposures, of course, also enhances very weak lines.

Many of the interstellar C iv and Si iv lines discussed below are at least as broad as the resolution, so that comparison with theoretical line profiles can be used to verify the column densities and Doppler parameters,  $b$ , derived from curve-of-growth analyses of the equivalent widths. The resolution is such that instrumental broadening must be taken into account explicitly. The theoretical line profile is the convolution

$$\Phi(\lambda) = \int_{-\infty}^{\infty} \phi(y)g(\lambda - y)dy,$$

of  $\phi$ , the intrinsic line shape function, and  $g$ , the instrumental response function. The instrumental response is assumed to be a Gaussian having a full-width at half-peak of  $\Delta\lambda = \lambda/R$ :

$$g(\lambda - \lambda_i) = A \exp(-2.77259z^2),$$

where  $z = (\lambda - \lambda_i)/\Delta\lambda$  and  $A = 0.93944/\Delta\lambda$ . The intrinsic line shape is

$$\phi(\lambda) = \exp(-\tau_\lambda),$$

and the optical depth,  $\tau_\lambda$ , is proportional to the Voigt function,  $K(x, y)$ ,

$$\tau_\lambda = 1.497 \times 10^{-15} Nf\lambda_0 K(x, y)/b.$$

The wavelength of the line center,  $\lambda_0$ , is in Å, and  $N$  and  $f$  are the column density (cm<sup>-2</sup>) in the lower state and the oscillator strength of the transition, respectively. The Doppler parameter  $b$  (km s<sup>-1</sup>) is related to the Doppler half-width

$$\alpha_D = \frac{\lambda_0}{c} (\ln 2)^{1/2} b = 2.7771 \times 10^{-6} \lambda_0 b.$$

The Voigt function is as defined by Armstrong (1967), and its arguments are

$$x = \frac{\lambda - \lambda_0}{\alpha_D} (\ln 2)^{1/2} \quad \text{and} \quad y = \frac{\alpha_L}{\alpha_D} (\ln 2)^{1/2},$$

where  $\alpha_L = \gamma/4\pi$  and  $\gamma$  is the inverse of the radiative lifetime of the upper state of the transition. Finally, the

best-fitted continuum intensity,  $I_c(\lambda)$ , is determined from the observed line, and the function

$$I(\lambda) = I_c(\lambda)[1 - \Phi(\lambda)],$$

can be compared directly with the observed line. The calculated profile is required to reproduce both the central depth of the line,  $I(\lambda_0)/I_c(\lambda_0)$ , and the equivalent width

$$W = \int_0^{\infty} \Phi(\lambda) d\lambda.$$

In practice, the central depth of a partially-resolved line at a specified value of  $W$  is sensitive to the value of  $b$  unless the line is so highly saturated that it goes to zero intensity, or unless the implicit assumption of a single velocity feature is inadequate. The assumption of single velocity features is potentially a serious weakness in the analysis, but it is unavoidable given the resolution of the instrument. The analysis in terms of single features will underestimate the column density and overestimate  $b$  if more than one component contributes to the absorption.

### III. RESULTS OF THE SURVEY

The characteristics of the lines examined in this survey are summarized in Table 3. Unfortunately, the resonance line of C III at  $\lambda 977$  is not accessible to *IUE* and the intersystem transition C III]  $2s^2\ ^1S_0 - 2p\ ^3P_1^0$  at  $1908.7\ \text{\AA}$  has a very small oscillator strength, so the concentrations of this ion are not well determined. The strong line of Si III at  $1206.5\ \text{\AA}$  cannot be observed at all toward the more highly-reddened stars because interstellar extinction and the broad wings of interstellar H I  $L\alpha$  do not admit any appreciable signal at that wavelength. The signal levels at the positions of N V  $\lambda\lambda 1238, 1242$  in many of our spectra are also quite low. It is important to recognize that the narrow lines of C IV and Si IV usually have broad stellar counterparts. In the spectra of hot stars undergoing mass loss, the interstellar features often reside in the emission wings of the broad stellar line profiles and can at least be detected. Interstellar lines of C IV and Si IV can

easily be lost altogether in the spectra of B stars lacking winds because they occur at the bottoms of the corresponding stellar absorption lines.

Figure 1 shows the narrow lines of C IV and Si IV in the spectrum of HD 46223, the star of earliest spectral type (O4) in the Rosette Nebula. Each line comes from the average of three separate spectra having a combined exposure time of 3 hours. The equivalent widths are rather well determined, and the doublet ratios and curves of growth imply  $b = 12.5\ \text{km s}^{-1}$  and column density  $N = 7.0 \times 10^{13}\ \text{cm}^{-2}$  for C IV and  $b = 10\ \text{km s}^{-1}$  and  $N = 1.1 \times 10^{14}\ \text{cm}^{-2}$  for Si IV. These results are in harmony with the comparisons of observed and theoretical line profiles. The solid curves in Figure 1 are the corresponding theoretical profiles calculated according to the procedure described in § IIc. That the value of  $b$  should be smaller for Si IV than for C IV is consistent with the notion that thermal Doppler broadening at  $T \approx 10^4\ \text{K}$  dominates the line width.

Table 4 contains the measured equivalent widths of the lines of C III], C IV, Si III, and Si IV. The final column lists an adopted stellar temperature thought to be appropriate for the stellar spectral classification. This temperature derives from the scale of Conti (1973) which is based upon a comparison between theoretical model atmospheres and observed intensity ratios of lines of He I and He II. Most of the stars in Table 3 are giants or supergiants and therefore have lower effective temperature than their spectral classmates on the main sequence. These temperatures are used in a qualitative way to characterize the energy distributions of the stars in the extreme ultraviolet in relation to model atmospheres. The determination of effective temperatures of early-type stars is a complex problem (see Conti 1973; Conti and Leep 1974; Brune, Mount, and Feldman 1979).

In Table 4, the uncertainties in the equivalent widths are indicated in three broad ranges that refer to  $2\sigma$  formal errors. Upper limits are entered as  $3\sigma$  errors. Several C III] lines appear at the level of  $1\sigma$  to  $3\sigma$ , but there are no statistically significant detections yet. Where no measurement or limit is provided, no

TABLE 3  
SPECTRAL LINES OF HIGHLY-IONIZED SPECIES

Species	Vacuum Wavelength ( $\text{\AA}$ )	Oscillator Strength	Reference
C III.....	1908.734	$1.81 \times 10^{-7}$	Laughlin <i>et al.</i> 1978 and references therein
C IV.....	1548.202	0.194	Morton and Smith 1973
	1550.774	0.097	Morton and Smith 1973
N V.....	1238.821	0.151	Morton and Smith 1973
	1242.804	0.0752	Morton and Smith 1973
Si III.....	1206.510	1.66	Morton and Smith 1973
Si IV.....	1393.755	0.528	Morton and Smith 1973
	1402.769	0.262	Morton and Smith 1973

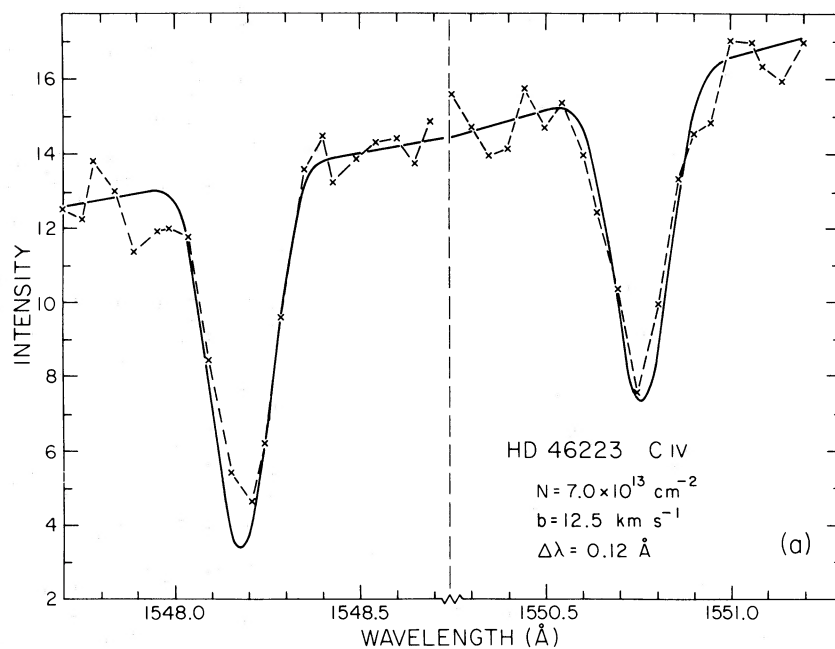


Fig. 1a

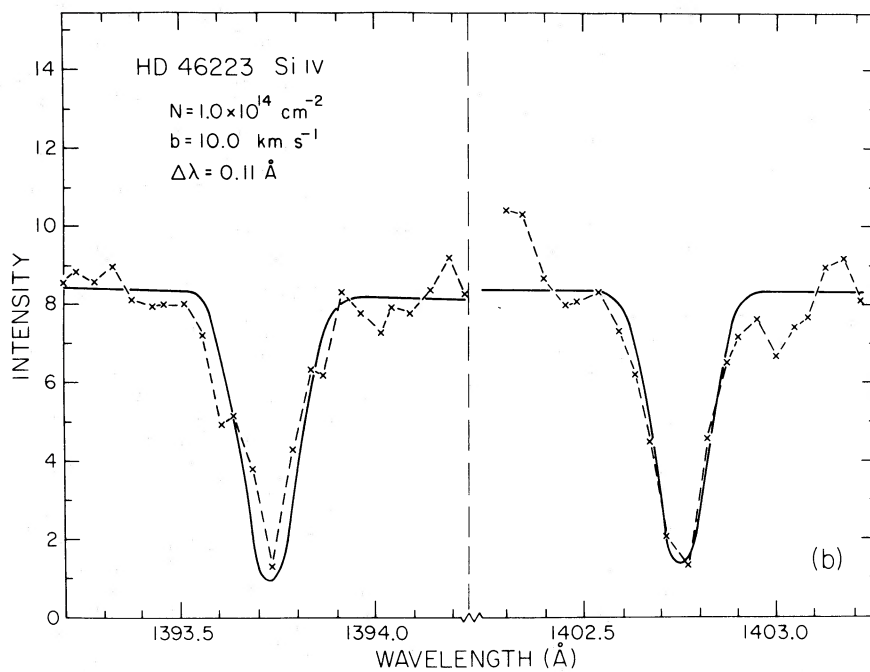


Fig. 1b

FIG. 1.—(a) Interstellar C iv lines  $\lambda\lambda 1548, 1550$  toward HD 46223. The solid curve is a theoretical profile with  $N(\text{C iv}) = 7.0 \times 10^{13} \text{ cm}^{-2}$  and  $b = 12.5 \text{ km s}^{-1}$ . (b) Interstellar Si iv lines  $\lambda\lambda 1393, 1402$  toward HD 46223. The solid curve is a theoretical profile with  $N(\text{Si iv}) = 1.0 \times 10^{14} \text{ cm}^{-2}$  and  $b = 10.0 \text{ km s}^{-1}$ .

TABLE 4  
MEASURED EQUIVALENT WIDTHS (Å)

HD NUMBER	C III] $\lambda 1908.7$	C IV		Si III $\lambda 1206.5$	Si IV		NUMBER OF EXPOSURES	STELLAR TEMPERATURE (K)
		$\lambda 1548.2$	$\lambda 1550.8$		$\lambda 1393.8$	$\lambda 1402.8$		
30614.....	<0.024	<0.02	<0.02	0.212 A <sup>b</sup>	<0.02	<0.02	1	30,000
36861.....	<0.027	...	...	0.44 B	...	...	1	33,000
38666.....	$\leq 0.027$	<0.03	<0.03	0.183 A	...	...	1	34,500
46223.....	$\leq 0.009$	0.140 A	0.097 A	...	0.156 A <sup>b</sup>	0.139 A <sup>b</sup>	3	40,000
57060.....	<0.009	0.102 A	0.046 A	0.229 A	0.090 A	0.063 A	4	32,000
57061.....	$\leq 0.027$	0.098 B	0.040 C	0.143 B	0.167 B	0.169 B	1	31,000
93250.....	$\leq 0.020$	0.581 <sup>b</sup>	0.384 <sup>b</sup>	...	0.901 <sup>b</sup>	0.670 <sup>b</sup>	2	50,000
148937.....	...	0.041 B <sup>b</sup>	$\leq 0.025^b$	...	...	...	1	37,000
149404.....	<0.014	0.036 B	0.024 C	...	...	0.058 C	3	31,000
151804.....	$\leq 0.018$	...	0.025 C	0.444 A	0.041 C	0.058 C	2	33,000
152424.....	...	...	0.044 B <sup>b</sup>	...	...	0.106 B <sup>b</sup>	1	31,000
203064.....	<0.027	0.049 B <sup>b</sup>	0.02 C <sup>b</sup>	0.247 A <sup>b</sup>	0.232 B <sup>b</sup>	0.118 B <sup>b</sup>	1	36,500
209975.....	<0.027	$\leq 0.05$	<0.05	$\leq 0.2$	0.096 B <sup>b</sup>	0.101 B <sup>b</sup>	1	30,000
213087.....	<0.03	<0.25	0.065 B	...	0.194 A	0.098 B	2	27,500

<sup>a</sup> Stars listed in Table 1 which are not listed here generally show no C IV or Si IV lines with equivalent widths exceeding 0.15 Å. Uncertainties: A (<10%), B (10–20%), C (>20%)—formal errors.

<sup>b</sup> Measurements may suffer from additional uncertainty due to use of an erroneous intensity-transfer function. Typically this uncertainty may be as large as 30% in equivalent width (see text).

meaningful value can be established because of confusion with stellar features or because the signal level is too low. Measurements subject to additional uncertainties resulting from processing with the erroneous intensity-transfer function are indicated in Table 4. These uncertainties are less than 30% except for the equivalent widths of C IV toward HD 152424 and of Si IV toward HD 203064, where the errors may be as large as 63%.

Stars listed in Table 1 but excluded from Table 4 show no narrow, obviously nonstellar lines of Si IV or C IV with equivalent widths exceeding 0.15 Å. The interstellar line profiles of HD 36861 and HD 93250 indicate complicated structure in radial velocity; aside from these two exceptions, the radial velocities of the highly-ionized species are similar to those of neutral and singly-ionized interstellar species. In most cases, the lines of C IV and Si IV are only partly resolved at the velocity resolution of 25 km s<sup>-1</sup>, and their strengths imply that the lines are saturated. The Si IV doublet ratios for HD 203064 and HD 213087 are close to the unsaturated values, but the equivalent widths are also large, suggesting either a large Doppler parameter,  $b \gtrsim 50$  km s<sup>-1</sup>, or (more likely) multiple velocity components toward these stars. For the other cases, with  $7.5 \leq b \leq 20$  km s<sup>-1</sup>, the derived column densities of C IV and Si IV lie in the range  $10^{13}$ – $10^{14}$  cm<sup>-2</sup>, and the ratios of column densities, Si IV/C IV range from 0.6 to 10.

In Table 5 we present the observations of interstellar lines of N V toward a few stars. In all cases these lines are weak. The equivalent widths are rather uncertain because of confusion with stellar features and inter-order scattered light. The column densities have been derived assuming that the N V lines are on the linear

part of the curve of growth. For those stars observed both in this survey and in the *Copernicus* survey of O VI, the column densities of O VI (Jenkins 1978a) are also tabulated. The ratio of column densities N V/O VI lies between 0.1 and 2.0, and no values greater than 1.0 have definitely been measured. Column densities of C IV and Si IV are also tabulated. These results assume  $b = 10$  km s<sup>-1</sup> for all directions except that toward HD 93250, where  $b = 50$  km s<sup>-1</sup> is adopted. In most cases, accurate column densities have not yet been established through careful profile fitting or curve-of-growth analysis; therefore, the values in Table 5 must be considered approximate.

Three of the lines of sight in Table 3 deserve further comment. The star HD 46223 lies in and contributes to the excitation of the Rosette Nebula. It shows an exceedingly rich interstellar absorption line spectrum including strong lines of neutrals such as C I, O I, and Mg I, as well as lines of ions that could be attributed to the prominent H II region. Eight bands in the fourth-positive system of CO can also be identified. The association of HD 46223 with a substantial H II region can be taken as strong circumstantial evidence that photoionized nebulae contribute to the C IV and Si IV absorption lines. The Doppler parameters determined for the C IV ( $b = 12.5$ ) and Si IV ( $b = 10$ ) lines are consistent with the measured widths of nebular lines of H and He at radio frequencies (Pedlar and Matthews 1973).

The star UW CMa (HD 57060) is a massive eclipsing binary system. Its orbital period is 4.39346 days and the velocity amplitude of the primary is 220 km s<sup>-1</sup>. If the narrow C IV and Si IV lines were formed in the atmosphere of one of the stars, they would be expected to exhibit periodic variations in radial velocity. Five

TABLE 5  
N V LINES AND COLUMN DENSITIES

STAR HD	EQUIVALENT WIDTH (Å)		N v	COLUMN DENSITIES ( $10^{13} \text{ cm}^{-2}$ )		
	$\lambda 1238$	$\lambda 1242$		O VI <sup>a</sup>	C IV	Si IV
13854.....	...	$\leq 0.050$	$\leq 4.9$	...	...	...
23180.....	...	$\leq 0.016$	$\leq 1.6$	...	...	...
30614.....	...	$< 0.030$	$< 2.0$	$< 2.5$	...	...
36861.....	$< 0.03$	$< 0.03$	$< 2.0$	1.62	...	...
36879.....	$< 0.03$	$< 0.03$	$< 2.0$	...	...	...
38666.....	0.018	$\leq 0.019$	0.9	6.6	...	...
41117.....	...	$\leq 0.03$	$\leq 3.0$	...	...	...
46223.....	0.085	0.036	3.8	...	8.3	11.0
57060.....	...	0.016	1.6	2.88	3.8	2.6
57061.....	0.030	0.025	2.5	3.31	3.1	19.0
91316.....	$< 0.04$	$< 0.03$	$< 3.0$	1.51	...	...
93250.....	0.040	0.027	2.3	...	29.0 <sup>b</sup>	78.0 <sup>b</sup>
112244.....	...	0.055:	5.3:	7.24	...	...
147933.....	$< 0.04$	$< 0.03$	$< 3.0$	...	...	...
148937.....	...	0.047	4.6	...	1.0	...
149404.....	...	$< 0.03$	$< 2.0$	...	1.1	1.7
151804.....	...	0.02	2.0	...	1.3	0.98
152424.....	...	$< 0.03$	$< 2.0$	...	2.6	4.9
203064.....	...	0.03	3.0	...	1.3	40.0
209975.....	$< 0.05$	$< 0.04$	$< 5.0$	...	$< 3.0$	2.9
212571.....	...	0.078:	7.6:	...	...	...
213087.....	$< 0.03$	$< 0.03$	$< 2.0$	...	4.4	13.0
218376.....	$< 0.02$	0.03:	3.0	...	...	...

<sup>a</sup> All column densities of O VI are from Jenkins (1978a).

<sup>b</sup> It has been assumed that  $b = 50$  to account approximately for the velocity structure in the profiles.

spectra of this system were obtained at relative phases  $\phi = 0.02, 0.22, 0.29,$  and  $0.52$  according to the ephemeris of Eaton (1978). Both C IV features are stationary with respect to the interstellar lines of Cl I  $\lambda 1347$  and Si II  $\lambda 1526$  within  $0.05 \text{ \AA}$  ( $10 \text{ km s}^{-1}$  in radial velocity) at all phases. A similar statement applies to the Si IV features. We conclude that these lines are truly interstellar. An O9 I star,  $\tau$  CMA (HD 57061) lies  $24'$  away from UW CMA (a projected separation of  $7 \text{ pc}$  at the adopted distance of  $1 \text{ kpc}$ ), and shows lines of C IV and Si IV of comparable strength and similar radial velocity. Both stars appear to be associated with the visible emission nebula S310.

HD 93250 is an O3 V star in the Carina Nebula near  $\eta$  Carinae (Walborn 1973; Conti and Frost 1977). The lines of C IV and Si IV are extremely strong and show multiple velocity components ranging from  $-150$  to  $+100 \text{ km s}^{-1}$ . The lines of Al III  $\lambda \lambda 1854, 1862 \text{ \AA}$  exhibit two of the same velocity components at about  $-60$  and  $-25 \text{ km s}^{-1}$ . The equivalent widths presented in Table 4 represent total absorption at all velocities. The details of these interstellar spectra will be discussed in a separate publication. The remarkable range of interstellar radial velocities in this direction has been noted previously by Walborn and Hesser (1975), Walborn (1975), Gardner *et al.* (1970), Dickel (1974), Deharvent and Maucherot (1975), and Huchtmeier and Day (1975).

#### IV. INTERPRETATION

##### a) General Considerations

When interstellar O VI lines were first observed widely with *Copernicus*, it was noted that measurements of interstellar C IV and Si IV might help determine the ionization structure and temperature of the gas responsible for the highly-ionized species (York 1974; Jenkins and Meloy 1974). It was also pointed out that H II regions around the stars of earliest spectral type should contain significant concentrations of C IV and Si IV. Our observations of C IV and Si IV are consistent with their formation by photoionization in normal H II regions (except for the star in the Carina Nebula); as a result, the C IV and Si IV lines provide no additional insight into the nature of the gas containing O VI. The fact that interstellar C IV and Si IV are observed only toward very hot stars in our sample is due in part to an observational selection effect: in cooler stars and in those that lack strong stellar winds, it is virtually impossible to recognize weak, narrow lines superposed on the strong stellar absorption lines. If oxygen, carbon, and silicon have approximately normal abundances, the lines of C IV and Si IV are far too strong to arise in gas at the temperatures  $T \gtrsim 10^5 \text{ K}$  required to produce the measured concentrations of O VI. The column density of Si IV is comparable to or greater than that of C IV in all



cases. If the abundances of silicon and carbon are similar to solar abundances, a collisionally-ionized gas would have to be at temperatures  $T \lesssim 50,000$  K in order to reproduce the observed ionization. It appears that neither hot coronal gas (Jenkins 1978*b*), nor stellar-wind "bubbles" (Weaver *et al.* 1977) can account for the observed amounts of both O VI and of C IV and Si IV.

It is very unlikely that ionization of predominantly neutral interstellar gas by cosmic rays or X-rays is responsible for the C IV and Si IV. Charge transfer between these ions and H is so rapid that prodigious ionization rates would be required (see Steigman 1975*a, b*). In a normal diffuse interstellar cloud, virtually all of the gas-phase carbon is  $C^+$  with a concentration  $n(C^+) \approx 3 \times 10^{-4} n$  in terms of the total density,  $n$ , of hydrogen nuclei. The  $C^{+3}$  ion can be produced by X-ray ionization of a K shell electron of  $C^+$  followed by radiationless Auger emission of a second electron at a rate  $\Gamma_x n(C^+) \text{ cm}^{-3} \text{ s}^{-1}$  (Weisheit and Dalgarno 1972; Weisheit 1973).  $C^{+3}$  is removed by charge transfer with H at a rate  $1.5 \times 10^{-9} n \text{ s}^{-1}$  (Watson and Christenson 1979), so that the equilibrium concentration of  $C^{+3}$  is simply  $n(C^{+3}) = 2 \times 10^5 \Gamma_x$ . The observations (Tables 1 and 4) indicate that a column density  $n(C^{+3})L \approx 3 \times 10^{13} \text{ cm}^{-2}$  can be found when the color excess  $E(B - V) = 2 \times 10^{-22} nL$  is 0.5 magnitudes or less. It follows that an ionization rate  $\Gamma_x \gtrsim 6 \times 10^{-14} n \text{ s}^{-1}$  would be required to maintain the observed  $C^{+3}$  in the predominantly neutral gas. At any reasonable density, this rate greatly exceeds the ionization rate due to the galactic X-ray background,  $\Gamma_x = 6 \times 10^{-17} \text{ s}^{-1}$ , calculated by Weisheit (1973).

The ionization of the interstellar gas might be affected by a nearby stellar X-ray source (McCray, Wright, and Hatchett 1977). Preliminary *IUE* observations of C IV and Si IV lines toward HD 153919, the O7 primary of an X-ray binary system, indicate the possibility of observing such effects directly (Dupree *et al.* 1978). Detailed analyses of the interstellar gas near several X-ray sources will be reported elsewhere.

#### b) Interstellar Lines from H II Regions

In order to verify that the observed column densities of C IV and Si IV can be produced by normal H II regions, simple models of nebular ionization structure have been constructed. The model nebulae are assumed to be ionization-bounded and to have constant electron temperatures  $T_e = 10^4$  K. The total density is constant and the ionization structure is calculated for H,  $H^+$ , He,  $He^+$ , C,  $C^+$ ,  $C^{+2}$ ,  $C^{+3}$ , Si,  $Si^+$ ,  $Si^{+2}$ ,  $Si^{+3}$ , and  $Si^{+4}$ . The rate of ionization of species  $i$  at distance  $r$  from a star of temperature  $T_*$  and radius  $R_*$  is approximately

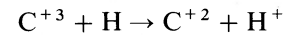
$$\Gamma_i \approx \left(\frac{R_*}{r}\right)^2 \exp(-\tau_i) \int_{\nu_i}^{\infty} \frac{\pi F_\nu(T_*)}{h\nu} \sigma_i(\nu) d\nu.$$

The emergent stellar flux  $F_\nu(T_*)$  has been taken from

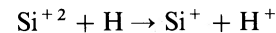
the atmosphere models of Kurucz (1979). Because most of the stars in Table 4 are giants or supergiants, models of low surface gravity have been used. The attenuation of ionizing photons due to continuous absorption by H and He is included in a very crude way through the opacity

$$\tau_i = N_H \sigma_H(\nu_i) + N_{He} \sigma_{He}(\nu_i),$$

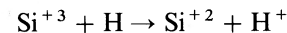
where  $N_H$  and  $N_{He}$  are the column densities of H and He, respectively, and the photoionization cross sections are evaluated at the threshold frequency of species  $i$ . Diffuse radiation in the nebula has been neglected. The cross sections for photoionization of the various stages of hydrogen, helium, and carbon are those collected from various sources by Osterbrock (1974). For Si and  $Si^+$ , we use the cross sections of Chapman and Henry (1972). For  $Si^{+2}$ ,  $Si^{+3}$ , and  $Si^{+4}$  we assume that the frequency dependences mimic those of He,  $C^{+3}$ , and Ne, respectively, and we estimate threshold cross sections according to the prescription of Gould (1978). The abundance of each species is computed as a function of  $r$  from the star to the classical Stromgren radius assuming balance between the rates of photoionization, radiative recombination, and charge transfer at every point. The column densities of all species are then evaluated by integration over path length. Rates of radiative recombination are those of Aldrovandi and Pequignot (1973). The following charge transfer processes have been included and are found to be significant:



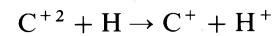
(Watson and Christenson 1979),



(McCarroll and Valiron 1976), and



(S. Butler, private communication). McCarroll and Valiron (1975) have shown that none of the possible charge transfer channels



is likely to be rapid. The model nebulae ignore possible effects of absorption of ionizing photons by dust. Internal dust will decrease the concentrations of highly-ionized species not only by competing directly for the photons that produce them, but also by increasing the concentrations of neutral H and He and thus augmenting the effect of charge transfers. H II regions like the Rosette Nebula have central cavities and differ in this respect from the models of uniform density. This may be a crucial factor in the abundances of  $C^{+3}$  and  $Si^{+3}$  because these species tend to have their greatest abundances nearest the exciting star. Many real nebulae also have more than one central star, so that the ionization structure might actually be governed largely by the ionizing flux from another nearby star that differs in spectral type from the one

being observed. The rates of photoionization at  $r = R_*$  and  $\tau_i = 0$  for several stellar models are presented in Table 6. Also listed are the corresponding total luminosities in hydrogen-ionizing photons,  $S_{50}/R_*^2$ , where  $S_{50}$  is in units of  $10^{50}$  photons  $s^{-1}$  and  $R_*$  is in solar radii. All the stellar models have negligible fluxes of photons capable of ionizing  $He^+$ ,  $C^{+3}$ , and  $Si^{+4}$ .

Having noted the above limitations of the models, we present the calculated results in Figure 2. Only the equivalent widths are directly measurable, therefore the figure shows the predicted equivalent widths as functions of stellar temperature for the lines of C IV and Si IV. The various curves indicate the sensitivity of the result to the Doppler parameter,  $b = 7.5$  and  $20 \text{ km s}^{-1}$ , and to the nebular electron density,  $n_e = 1.0$  and  $1000.0 \text{ cm}^{-3}$ . For comparison, the observations are presented in Figure 2 at the adopted effective temperatures given in Table 4. In no case are there serious disagreements between the observed line strengths and those predicted by simple models. The only discrepant point is due to the line of sight to 26 Cep (HD 213087). It is possible that the effective temperature of this star has been underestimated or that there is another, hotter source of ionization of the nearby H II region S150. The heliocentric radial velocity of 26 Cep is  $-14.7 \text{ km s}^{-1}$ , while the velocities of nearby members of the associations Cep OB1 and Cep OB5 are  $-50$  to  $-60 \text{ km s}^{-1}$ . Although an accurate absolute velocity scale has not yet been established for these data, the interstellar lines of Si II show two velocity components separated by almost  $50 \text{ km s}^{-1}$ , and the C IV is associated with the more highly blueshifted of these, suggesting that the highly-ionized material may not be so directly associated with 26 Cep itself. The observed points lying below and to the right of the theoretical curves in Figure 2 can easily be explained by the limitations of the models or by depletion of carbon and silicon below the assumed abundances of  $3.7 \times 10^{-4}$  and  $3.5 \times 10^{-5}$ , respectively, relative to hydrogen.

It is worth noting that the lines of sight to five O stars, HD 30614, 36861, 36879, 38666, and 112244, do not contain detectable amounts of C IV or Si IV. Four of these stars, HD 30614, 38666, 36879, and 112244 are not associated with any prominent visible nebulosity, and it is likely that the density of any associated nebula is too low to support observable column densities of the highly-ionized species. The star HD 36861 ionizes

the large nebula S264 which has a low average density of about  $2 \text{ cm}^{-3}$ . Figure 2 indicates that in nebulae of very low density, the column densities of the highly-ionized species are not always large enough to be detected, even though the exciting star may be of early spectral type. In a classical Strömgren sphere, the total column density of ions varies with density as  $n_e R \propto n_e^{1/3}$ ; thus the denser nebulae will contain greater column densities of all ions for a given type of exciting star. Harms, Strittmatter, and Williams (1978) have used observations of nebular emission line intensities to infer the ultraviolet ionizing flux emitted by HD 36861.

Figure 3 presents the calculated equivalent widths in Si III  $\lambda 1206.5 \text{ \AA}$ . The upper limits to C III abundances from the weak intersystem transition do not place any useful constraints upon the models, although a *bona fide* measurement at the level of the present limits would certainly do so.

In many cases, the properties of these H II regions (especially electron density) are not known from other observations. Studies of interstellar absorption lines such as Si III, Si IV, and C IV can provide useful information about the ionization structures of such nebulae.

### c) Complementary Visible Observations

It may be possible in some directions to separate the contributions of nebulae and neutral clouds to the column densities of such ions as C II and Si II. It is also possible to infer the emission measure,  $E = \int n_e^2 dr$ , from observations of nebular absorption lines of metastable He I ( $2^3S$ ). In a low density nebula, the concentration of He ( $2^3S$ ) is given to a good approximation by

$$n(2^3S) \approx \frac{n_e n_{He} + \alpha(2^3S)}{A(2^3S-1^1S)},$$

(Drake and Robbins 1972) where  $\alpha(2^3S)$  is the effective rate coefficient for recombination and cascade leading to population of  $2^3S$ , and  $A(2^3S-1^1S) = 1.27 \times 10^{-4} \text{ s}^{-1}$  is the probability of the magnetic dipole transition to the ground state (Drake 1971). As an example, at  $T_e = 10^4 \text{ K}$ ,  $\alpha(2^3S) = 2.1 \times 10^{-13} \text{ cm}^3 \text{ s}^{-1}$ , so that

$$n(2^3S) = 1.65 \times 10^{-9} n_e n_{He^+}.$$

TABLE 6  
RATES OF PHOTOIONIZATION

$T_*$	$S_{50}/R_*^2$	H	He	C	C <sup>+</sup>	C <sup>+2</sup>	Si	Si <sup>+</sup>	Si <sup>+2</sup>	Si <sup>+3</sup>
25000	9.54 (-6)	7.88 (+4)	4.93 (+1)	7.77 (+5)	3.39 (+1)	1.82 (-8)	9.60 (+6)	2.07 (+3)	1.20 (-3)	5.28 (-8)
30000	6.63 (-5)	4.82 (+5)	5.16 (+3)	3.17 (+6)	3.30 (+3)	4.64 (-4)	2.41 (+7)	2.70 (+4)	2.82	9.34 (-4)
35000	3.96 (-4)	2.37 (+6)	2.84 (+5)	1.12 (+7)	1.63 (+5)	5.96 (-1)	4.92 (+7)	2.08 (+5)	4.25 (+3)	1.28 (0)
40000	9.59 (-4)	5.01 (+6)	1.50 (+6)	2.30 (+7)	8.25 (+5)	1.01 (+1)	7.54 (+7)	5.14 (+5)	5.37 (+4)	2.08 (+1)

NOTE.—The number in parenthesis is the power of 10 by which the number preceding it is to be multiplied.

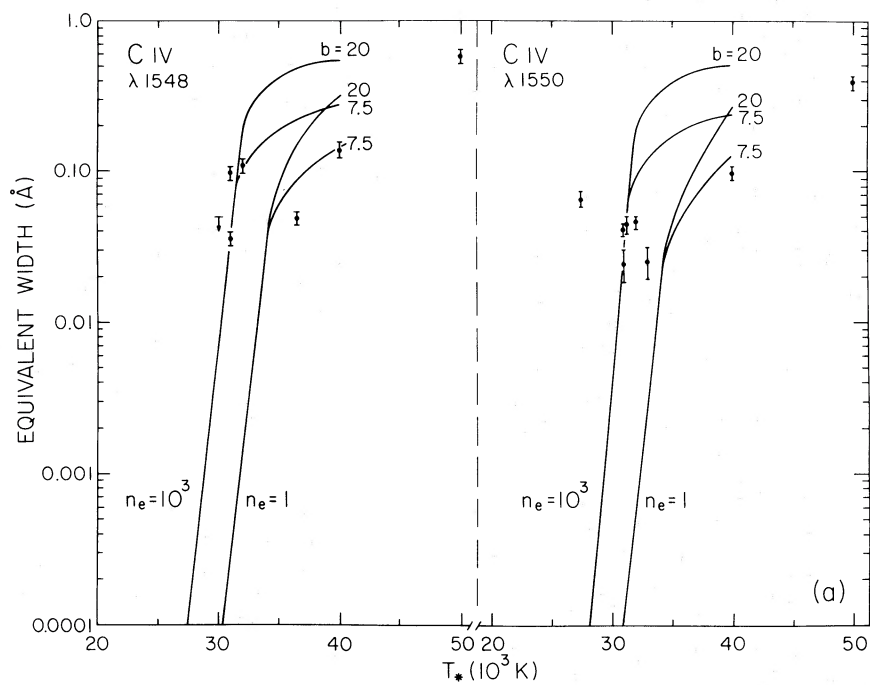


FIG. 2a

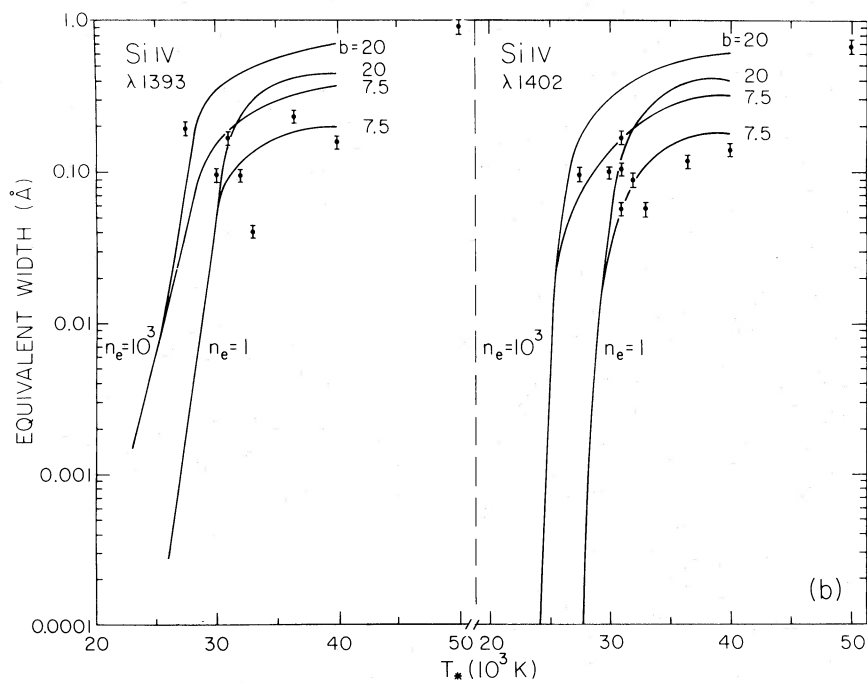


FIG. 2b

FIG. 2.—(a) Equivalent widths of C IV lines as functions of stellar temperature predicted for model nebulae. Different curves indicate the allowed range of equivalent widths for electron densities between  $1 \text{ cm}^{-3}$  and  $1000 \text{ cm}^{-3}$ , and Doppler parameters  $7.5 \leq b \leq 20 \text{ km s}^{-1}$ . Observed values are indicated by open circles. (b) Equivalent widths of Si IV lines as in Fig. 2a.

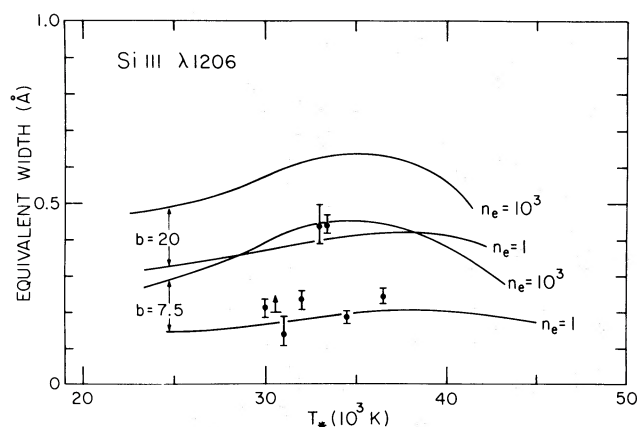


FIG. 3.—Equivalent width of Si III  $\lambda 1206.5$  for model nebulae, as in Figs. 2a and 2b.

Because  $n_{\text{He}^+} \approx 0.1 n_e \chi$ , the column density

$$N(2^3S) \approx 1.65 \times 10^{-10} E \chi,$$

where  $E$  is the emission measure in  $\text{cm}^{-5}$ , and  $\chi$  is a correction factor related to the ratio of radii of the ionization zones of  $\text{H}^+$  and  $\text{He}^+$  (see Rubin 1968). In the weak-line limit, the equivalent width of a line of oscillator strength  $f$  and wavelength  $\lambda$  in  $\text{\AA}$  arising in  $\text{He I } (2^3S)$  is

$$W \approx 4.5 \times 10^{-9} E \lambda^2 f \text{ m}\text{\AA},$$

where  $E$  is now in the conventional units of  $\text{cm}^{-6}$  pc. Radio observations of the Rosette Nebula indicate  $E \approx 2600 \text{ cm}^{-6}$  pc (Pedlar and Matthews 1973), which implies an equivalent width in  $\text{He I } \lambda 3889$  of  $W = 11 \text{ m}\text{\AA}$  toward HD 46223. If the nebula is inhomogeneous on scales smaller than the antenna beam size for the radio observations, such lines could be even stronger. A survey of nebular absorption lines  $\text{He I } \lambda 3889$  or  $\lambda 10830$  toward exciting stars of faint nebulae would be of considerable value.

#### d) Conclusions

Strong interstellar C IV and Si IV lines in our sample are always seen toward stars having stellar winds with large terminal velocities. There is however no discernible pattern or correlation of line strength with stellar wind velocity. Moreover, as shown by comparison of the data in Tables 1 and 3, high velocity in a stellar

wind does not automatically imply the presence of strong lines of interstellar Si IV and C IV. As demonstrated by Snow and Morton (1976), strong stellar winds tend to be correlated with stellar luminosity. The hottest, most luminous stars also support the most extensive and most highly-ionized H II regions. It will of course be important to determine whether careful analysis of ultraviolet spectra can reveal features attributable to the interaction of stellar winds with surrounding nebulae. Huber *et al.* (1979) have recently presented *IUE* observations of highly-ionized species toward the Wolf-Rayet star HD 192163 and its associated nebula NGC 6888. The profiles of interstellar C IV and Si IV in this direction show two distinct velocity components. One of the components is blue-shifted by about  $90 \text{ km s}^{-1}$  with respect to the other interstellar lines, and it may be formed in the region of interaction between the stellar wind and ambient interstellar gas. No shifted velocity features appear in our spectra of O and B stars, except for the case of HD 93250.

In conclusion, we have presented new data on interstellar absorption lines of highly-ionized species C III, C IV, N V, Si III, and Si IV, and on stellar wind velocities. The strengths of the lines of carbon and silicon are consistent with their formation in normal ionized nebulae around the hot stars toward which they are observed. Simple models of the ionization structures of H II regions were constructed for comparison with the observations. More analyses of such nebular absorption lines will help elucidate the ionization structures of H II regions. The interstellar lines of N V may be related to the widely observed O VI lines attributed to hot, collisionally-ionized gas.

This work was begun while one of us (J. H. B.) was at the University of Minnesota, and it was supported by NASA grant NSG-5237 there, and by NSG-5380 and NSG 7176 at Harvard College Observatory.

The observations reported above were made possible by the efforts of a vast number of people associated with the *IUE* project. We are particularly grateful to the *IUE* resident astronomers, Drs. C.-C. Wu, A. V. Holm, and F. H. Schiffer, to the telescope operators, and to the image-processing team for their direct contributions to this work.

We thank Professor A. Dalgarno for a critical reading of the manuscript. We are grateful to Dr. K. S. de Boer for helpful comments.

#### REFERENCES

- Aldrovandi, S. M. V., and Pequignot, D. 1973, *Astr. Ap.*, **25**, 137.  
 Armstrong, B. H. 1967, *J. Quant. Spectrosc. Rad. Transf.*, **7**, 61.  
 Boggess, A., *et al.* 1978a, *Nature*, **275**, 372.  
 ———. 1978b, *Nature*, **275**, 377.  
 Bruhweiler, F. C., Kondo, Y., and McCluskey, G. E. 1979, *Ap. J. (Letters)*, **229**, L39.  
 Brune, W. H., Mount, G. H., and Felman, P. D. 1979, *Ap. J.*, **227**, 884.  
 Burstein, P., Borken, R. J., Kraushaar, W. L., and Sanders, W. T. 1977, *Ap. J.*, **213**, 405.  
 Castor, J., McCray, R., and Weaver, R. 1975, *Ap. J. (Letters)*, **200**, L107.  
 Chapman, R. D., and Henry, R. J. W. 1972, *Ap. J.*, **173**, 243.  
 Cohn, H., and York, D. G. 1977, *Ap. J.*, **216**, 408.  
 Conti, P. S. 1973, *Ap. J.*, **179**, 181.  
 Conti, P. S., and Frost, S. A. 1977, *Ap. J.*, **212**, 728.  
 Conti, P. S., and Leep, E. M. 1974, *Ap. J.*, **193**, 113.  
 Cowie, L. L., Jenkins, E. B., Songaila, A., and York, D. G. 1979, *Ap. J.*, **232**, 467.  
 Cowie, L. L., Songaila, A., and York, D. G. 1979, *Ap. J.*, **230**, 469.

- Cowie, L. L., and York, D. G. 1978a, *Ap. J.*, **220**, 129.  
 ———. 1978b, *Ap. J.*, **223**, 876.
- Cox, D. P., and Smith, B. W. 1974, *Ap. J. (Letters)*, **189**, L105.
- Deharveng, L., and Maucherat, M. 1975, *Astr. Ap.*, **41**, 27.
- Dickel, H. R. 1974, *Astr. Ap.*, **31**, 11.
- Drake, G. W. F. 1971, *Phys. Rev.*, **A3**, 908.
- Drake, G. W. F., and Robbins, R. R. 1972, *Ap. J.*, **171**, 55.
- Dupree, A. K. et al. 1978, *Nature*, **275**, 400.
- Eaton, J. A. 1978, *Ap. J.*, **220**, 582.
- Gardner, F. F., Milne, D. K., Mezger, P. G., and Wilson, T. L. 1970, *Astr. Ap.*, **7**, 349.
- Gould, R. J. 1978, *Ap. J.*, **219**, 250.
- Harms, R. J., Strittmatter, P. A., and Williams, R. E. 1978, *Ap. J.*, **223**, 234.
- Huber, M. C. E., Nussbaumer, H., Smith, L. J., Willis, A. J., and Wilson, R. 1979, *Nature*, **278**, 697.
- Huchtmeier, W. K., and Day, G. A. 1975, *Astr. Ap.*, **41**, 153.
- Jenkins, E. B. 1977, in *Topics in Interstellar Matter*, ed. H. Van Woerden (Dordrecht: D. Reidel), pp. 3, 5, 45.
- Jenkins, E. B. 1978a, *Ap. J.*, **219**, 845.  
 ———. 1978b, *Ap. J.*, **220**, 107.  
 ———. 1978c, *Comments Ap.*, **7**, 121.
- Jenkins, E. B., and Meloy, D. A., 1974, *Ap. J. (Letters)*, **193**, L121.
- Kurucz, R. L. 1979, *Ap. J. Suppl.*, **40**, 1.
- Laughlin, C., Constantinides, E. R., and Victor, G. A. 1978, *J. Phys. B.*, **11**, 2243.
- McCarroll, R., and Valiron, P. 1975, *Astr. Ap.*, **44**, 465.  
 ———. 1976, *Astr. Ap.*, **53**, 83.
- McCray, R. 1977, in *Topics in Interstellar Matter*, ed. H. Van Woerden (Dordrecht: Reidel), p. 35.
- McCray, R., Wright, C., and Hatchett, S. 1977, *Ap. J. (Letters)*, **211**, L29.
- McKee, C. F. 1977, in *Topics in Interstellar Matter*, ed. H. Van Woerden (Dordrecht: Reidel), p. 27.
- McKee, C. F., and Cowie, L. L. 1977a, *Ap. J.*, **211**, 135.  
 ———. 1977b, *Ap. J.*, **215**, 213.
- McKee, C. F., and Ostriker, J. P. 1977, *Ap. J.*, **218**, 148.
- Morton, D. C., and Smith, W. H. 1973, *Ap. J. Suppl.*, **26**, 333.
- Osterbrock, D. E. 1974, *Astrophysics of Gaseous Nebulae*, (San Francisco: Freeman), p. 311 ff.
- Pedlar, A., and Matthews, H. E. 1973, *M.N.R.A.S.*, **165**, 381.
- Rogerson, J. B., York, D. G., Drake, J. F., Jenkins, E. B., Morton, D. C., and Spitzer, L. 1973, *Ap. J. (Letters)*, **181**, L110.
- Rubin, R. H. 1968, *Ap. J.*, **153**, 761.
- Savage, B. D., and de Boer, K. S. 1979, *Ap. J. (Letters)*, **230**, L37.
- Smith, B. W. 1977, *Ap. J.*, **211**, 404.
- Snow, T. P., and Morton, D. C. 1976, *Ap. J. Suppl.*, **32**, 429.
- Steigman, G. 1975a, *Ap. J. (Letters)*, **195**, L39.  
 ———. 1975b, *Ap. J.*, **199**, 642.
- Walborn, N. R. 1973, *Ap. J.*, **179**, 517.  
 ———. 1975, *Ap. J. (Letters)*, **202**, L129.
- Walborn, N. R., and Hesser, J. E. 1975, *Ap. J.*, **199**, 535.
- Watson, W. D., and Christensen, R. B. 1979, *Ap. J.*, **231**, 627.
- Weaver, R., McCray, R., Castor, J., Shapiro, P., and Moore, R. 1977, *Ap. J.*, **218**, 377; 1978, **220**, 742.
- Weisheit, J. C. 1973, *Ap. J.*, **185**, 877.
- Weisheit, J. C., and Dalgarno, A. 1972, *Ap. Letters*, **12**, 103.
- York, D. G. 1974, *Ap. J. (Letters)*, **193**, L127.

J. H. BLACK, A. K. DUPREE, L. W. HARTMANN, and J. C. RAYMOND: Center for Astrophysics, 60 Garden Street, Cambridge, MA 02138